

# Adaptive Information Bottleneck Guided Joint Source-Channel Coding

Lunan Sun<sup>1</sup>, Caili Guo<sup>1</sup>, and Yang Yang<sup>1</sup>

<sup>1</sup>Beijing University of Posts and Telecommunications

## ABSTRACT

Joint source channel coding (JSCC) has attracted increasing attentions due to its robustness and high efficiency. However, the existing research on JSCC mainly focuses on minimizing the distortion between the transmitted and received information, while limiting the required data rate. Therefore, even though the transmitted information is well recovered, the transmitted bits may be far more than the minimal threshold according to the rate-distortion (RD) theory. In this paper, we propose an adaptive Information Bottleneck (IB) guided JSCC (AIB-JSCC), which aims at achieving the theoretically maximal compression ratio for a given reconstruction quality. In particular, we first derive a mathematically tractable form of loss function for AIB-JSCC. To keep a better tradeoff between compression and reconstruction quality, we further propose an adaptive algorithm that adjusts hyperparameter  $\beta$  of the proposed loss function dynamically according to the distortion during training. Experiment results show that AIB-JSCC can significantly reduce the required amount of the transmitted data and improve the reconstruction quality and downstream artificial-intelligent task performance.

## Introduction

Shannon’s information theorem lays the foundation of communications. In particular, based on Shannon’s theorem, it is optimal to separate the source compression and the channel error correction for a memoryless communication channel if the latency, complexity, and code length are not constrained<sup>1</sup>. However, the separate source channel coding (SSCC) is subject to several practical limitations. First, the infinite code length is impossible in practice, and SSCC becomes sub-optimal in this situation. In addition, to achieve theoretically optimal performance, maximum likelihood detection must be used, which is in general NP-hard<sup>2</sup>. This puts forward high requirements for computation complexity, and may lead to unacceptable latency. Furthermore, the future sixth generation (6G) network will connect trillion-level devices and require 10 to 1000 times higher data capacity<sup>3</sup>. In addition, 6G should support a wide range of services and applications, such as augmented reality, medical imaging and autonomous vehicles, which has strict latency requirement<sup>4</sup>. Therefore, SSCC is hard to meet the requirements of 6G.

To address the above-mentioned challenges, joint source-channel coding (JSCC) has attracted increasing attentions. The studies on JSCC can be classified into two types: the traditional research based on mathematical models and the deep learning (DL)-based research. The traditional research mainly focuses on performance analysis under ideal channel or source assumption<sup>5,6</sup>. The coding schemes, such as bit allocation algorithm<sup>7</sup>, robust nonlinear block coding<sup>8</sup>, etc. have been also studied. However, these hand-crafted coding schemes may require additional tuning. Motivated by the impressive performance of DL in many domains, DL-based JSCC have been extensively studied. The main goal of DL-based approaches is preserving information to improve the reconstruction quality. In particular, minimizing the mean-squared error (MSE) between the input and output<sup>9-11</sup> is the most general method to achieve this goal. In particular, Bourtsoulatze et al proposed a JSCC architecture called Deep JSCC that minimizes the MSE between the original image and the recovered image<sup>9</sup>. The proposed architecture outperforms SSCC that combines JPEG<sup>12</sup> or JPEG2000<sup>13</sup> with capacity-achieving channel codes. Kurka et al<sup>10</sup> and Xu et al<sup>11</sup> further improved the reconstruction quality of Deep JSCC by incorporating the channel output feedback and using channel-wise soft attention network, respectively. Besides, maximizing mutual information can also realize the preservation of information<sup>14,15</sup>. For instance, Choi et al proposed a discrete variational autoencoder model called Neural Error Correcting and Source Trimming (NECST), which can maximize the mutual information<sup>16</sup> between the source and noisy codewords<sup>14</sup>. Song et al developed a JSCC model called Infomax Adversarial-Bit-Flip (IABF)<sup>15</sup>. They further maximized the mutual information between the code and input image by adding it to the loss function.

Overall, the existing works on JSCC aim at minimizing the recovery distortion between the transmitted and received information by utilizing various distortion metrics as loss function while limiting the required data rate to a constant upper bound. Therefore, the transmitted data rate may be much larger than the minimal data rate given by the rate-distortion (RD) theory, thus a new form of JSCC is required to simultaneously consider the rate and the distortion.

However, the classical RD theory does seldom provide the explicit form of distortion function. To circumvent this challenge,

Tishby considered the mutual information between the codewords and the labels of the inputs as distortion, and proposed a specific form of RD theory coined as: Information bottleneck (IB) principle<sup>17</sup>, which already has an extensive applications<sup>18,19,20</sup>. Since IB inherits the properties of RD theory, it can obtain the maximal compression ratio and the optimal features in theory<sup>21,22</sup>. Therefore, this work proposes IB guided JSCC to improve the compression ratio as much as possible for a given reconstruction quality. However, to apply IB principle into JSCC, two key issues must be solved:

*Question 1: Since the classical form of IB is particularly designed for supervised tasks, how to design a proper and tractable form of IB for a JSCC system?*

*Question 2: How to choose a proper value of hyperparameter  $\beta$  of IB to trade off compression and reconstruction quality?*

In this paper, we propose an adaptive IB guided JSCC (AIB-JSCC) scheme to solve these two questions, which aims at reducing the transmission bits while guaranteeing the reconstruction quality. To the best of authors' knowledge, this is the first work that applies IB into JSCC, and provides a theoretically maximal compression ratio guidance for neural network. In particular, we first derive a mathematically tractable form of IB objective for AIB-JSCC via variational lower bound and contrastive log-ratio upper bound (CLUB) of mutual information. To balance compression and reconstruction quality, a hyperparameter  $\beta$  is introduced into the proposed IB objective. We further develop an adaptive algorithm to adjust the value of  $\beta$  dynamically by exploiting the reconstruction error. The experimental results show that the AIB-JSCC can obtain higher reconstruction quality with only 5% and 80% bits that SSCC and IABF need. Overall, the proposed scheme has significantly reduced the required storage space and the amount of transmitted data, which is particularly suitable for 6G communications. The contributions of the paper can be summarized as:

1. We develop a new mathematically tractable and differentiable form of IB objective that can simultaneously minimize the reconstruction distortion and the transmission rate of the JSCC system.
2. We propose an adaptive algorithm, which can adjust hyperparameter  $\beta$  of the proposed IB objective to balance the reconstruction distortion and the transmission rate.
3. We compare the proposed schemes with state-of-the-art JSCC methods and quantify the performance gain.

## Methods

After introducing the motivation of our work in this section, we derive the proposed IB objective for the JSCC system.

We then present the adaptive IB algorithm, including the upper bound of  $\beta$  and the application of the proposed algorithm. AIB-JSCC combines the proposed IB objective and the adaptive IB algorithm as depicted in Figure 1. We first train the encoder and decoder jointly by optimizing the proposed IB objective. Then, we apply the proposed adaptive IB algorithm to adjust hyperparameter  $\beta$ . Finally, we alternately change  $\beta$  and train the network.

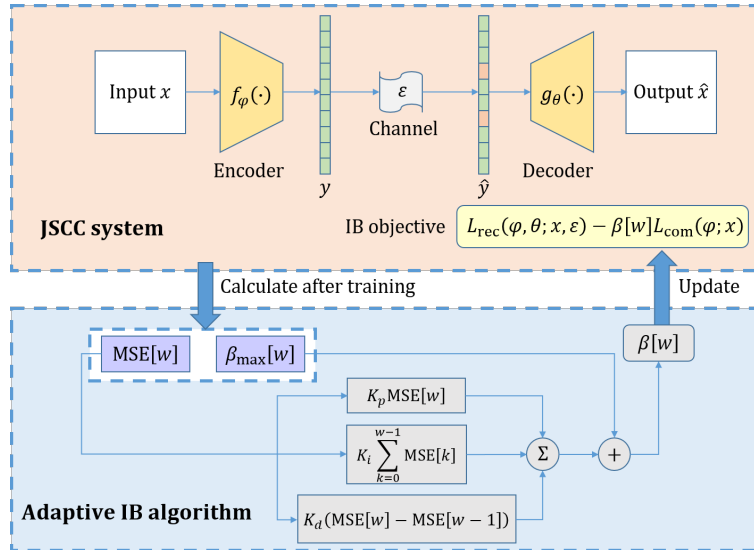


**Figure 1.** An illustration of our proposed AIB-JSCC. Orange: JSCC system with the proposed IB objective. Blue: adaptive IB algorithm. First, we train the JSCC system which consists of an autoencoder, by optimizing the proposed IB objective. Then, we adjust  $\beta$  according to the proposed algorithm. Finally, we alternately change  $\beta$  and train the network.

## Motivation

The existing JSCC works are mostly theoretically guided by the classical RD theory. The RD theory determines the required information rate of the input in terms of the rate distortion function  $R(D)$ , given the expected distortion  $D$ . Denote  $X$  as the input random variable and  $Y$  as the codewords of  $X$ . Then RD function is defined as,

$$R(D) = \inf_{\{p(Y|X): \langle d(X,Y) \rangle \leq D\}} I(X,Y), \quad (1)$$

where  $d(X,Y)$  is the distortion function,  $p(Y|X)$  is the conditional probability of  $Y$  given  $X$ ,  $D$  is the maximum tolerable average distortion, and  $I(X,Y)$  is the mutual information between  $X$  and  $Y$ , which is regarded as the required transmitted information rate in information theory<sup>1</sup>. The goal of RD theory is to obtain a proper  $Y$  that minimizes the rate  $I(X,Y)$  with given  $d(\cdot)$ . Introducing a Lagrange multiplier  $\beta$  into Eq. (1), we have

$$\min_{p(Y|X)} I(X,Y) + \beta d(X,Y). \quad (2)$$

Since  $I(X,Y) = H(X) - H(X|Y)$  and  $H(X|Y) \geq 0$ ,  $I(X,Y) \leq H(X)$ . Replacing  $I(X,Y)$  by its upper bound  $H(X)$ , the optimization problem of Eq. (2) can be simplified as,

$$\min_{p(Y|X)} H(X) + \beta d(X,Y). \quad (3)$$

In the existing works on JSCC,  $X$  is usually input images and its entropy  $H(X)$  is a constant that cannot be optimized by the network<sup>18</sup>. Therefore, Eq. (3) can be further simplified into

$$\min_{p(Y|X)} d(X,Y). \quad (4)$$

Eq. (4) is the loss function of the existing JSCC works. However, Eq. (4) does not minimize the rate  $I(X,Y)$  since  $I(X,Y)$  is replaced by a constant  $H(X)$ , which is further neglected in Eq. (4). Therefore, rate  $I(X,Y)$  of the existing works can be much larger than the theoretical minimum value according to RD theory. This motivates us to design a new loss function that can optimize the distortion  $d(X,Y)$  and the rate  $I(X,Y)$  simultaneously following the RD theory.

Nevertheless, RD theory does not specify the concrete form of  $d(\cdot)$ . To extract the contained information of a target random variable  $Z$  in input  $X$ , Tishby proposed to use the mutual information between  $Y$  and  $Z$ ,  $I(Y,Z)$  as  $-d(\cdot)$  and extended Eq. (1) into IB principle<sup>21</sup>. Since  $Y = Y(X)$  is a function of  $X$ , there exists a Markov chain  $Z \leftrightarrow X \leftrightarrow Y$ <sup>23</sup>. Denote  $p(X,Z)$  as the joint distribution of input  $X$  and target  $Z$ . The goal of IB principle is to find a  $Y$  that minimizes the mutual information  $I(X,Y)$ , while the mutual information  $I(Y,Z)$  must be greater than a certain threshold  $I_c$ , and we have

$$\begin{aligned} & \inf_{p(Y|X)} I(X,Y) \\ & \text{subject to: } I(Y,Z) \geq I_c. \end{aligned} \quad (5)$$

Introducing a Lagrange multiplier  $\beta$  into Eq. (5), we have

$$\max_{p(Y|X)} I(Y,Z) - \beta I(X,Y). \quad (6)$$

Equation (6) is the basic form of IB principle. The first term in Eq. (6) encourages  $Y$  to be predictive of  $Z$ , and the second term in Eq. (6) encourages  $Y$  to compress the information related to  $X$ . Hyperparameter  $\beta (> 0)$  tunes the tradeoff between prediction and compression. IB principle provides an approximation of minimal sufficient statistic (MSS)<sup>23</sup> by capturing the relevant information and compressing the redundant parts. By tuning  $\beta$ , IB principle can guide the system to obtain the optimal features that are maximally compressed<sup>22</sup>. The most common application of IB principle is the loss function of supervised tasks, where  $X$  is the input,  $Y$  is the embedding output, and  $Z$  is the label of input<sup>18,24,25</sup>.

Even though IB principle defines a specific form of distortion and rate, and can be the guidance of the optimal features, the traditional IB form Eq. (6) is designed for supervised learning, and thus cannot be applied in JSCC directly. Moreover, the value of  $\beta$  is crucial to the performance, and thus the value of  $\beta$  needs to be properly optimized. To solve these problems, we first propose a new form of IB objective which is mathematically tractable and differentiable in the JSCC system. Then, we further propose an adaptive IB algorithm to adjust the value of  $\beta$  according to the distortion during training.

## IB objective for JSCC system

This section introduces our proposed IB objective and applies it in the JSCC system. Consider an image transmission system, which is an important and common communication scenario<sup>9,10,11,14,15</sup>. The system consists of an autoencoder, where the encoder and decoder are composed of neural network with parameters  $\varphi$  and  $\theta$ , respectively. Let  $x$ ,  $y$ ,  $\hat{y}$ ,  $\hat{x}$  represent the input, codeword, noisy codeword and reconstruction, respectively. We will learn a probabilistic encoder  $p_{\text{enc}}(y|x; \varphi)$  that can obtain codewords with the least amount of information and the best reconstruction quality. Since IB principle can guide the system to achieve theoretically maximal compression ratio with a certain tasks distortion, this work proposes an IB guided JSCC. However, the traditional form of IB principle shown as Eq. (6) is not applicable to the considered system since image transmission without label is unsupervised. To overcome this problem, we propose a new form of IB principle as follows:

$$\max_{\varphi, \theta} I(x, \hat{y}) - \beta I(x, y). \quad (7)$$

Similar to Eq. (6), the first term in Eq. (7) guarantees that the noisy codeword,  $\hat{y}$ , contains sufficient information to recover input  $x$  without distortion. However, solely maximizing  $I(x, \hat{y})$  may result in severe information redundancy in  $y$  and lead to overfitting. Thus, we use the second term to compress the information in  $y$  and act as a regularizer. These two terms in Eq. (7) closely interact with each other. By selecting a proper hyperparameter  $\beta$ , the JSCC system can accurately transmit images while minimizing the required transmission data amount.

However, the proposed IB objective in Eq. (7) cannot be applied in the JSCC systems directly since the mutual information  $I(x, y)$  and  $I(x, \hat{y})$  in Eq. (7) are mathematically intractable. To circumvent this challenge, we derive the variational lower bound of  $I(x, y)$  and estimates the upper bound of  $I(x, \hat{y})$  instead. In particular, for  $I(x, \hat{y})$ , we have

$$I(x, \hat{y}) = H(x) - H(x|\hat{y}) = H(x) + E_{x \sim p_{\text{data}}(x)} E_{\hat{y} \sim p(\hat{y}|x; \varphi)} [\log p(x|\hat{y}; \theta)], \quad (8)$$

where  $H(x)$  is a positive constant and cannot be optimized by the neural network. Therefore, maximizing  $I(x, \hat{y})$  is equal to maximizing its lower bound,  $E_{x \sim p_{\text{data}}(x)} E_{\hat{y} \sim p(\hat{y}|x; \varphi)} [\log p(x|\hat{y}; \theta)]$ .  $p_{\text{dec}}(\hat{x}|\hat{y}; \theta)$  is applied as a variational approximation of true posterior  $p(x|\hat{y})$ <sup>14</sup>,

$$\max I(x, \hat{y}) \triangleq \max E_{x \sim p_{\text{data}}(x)} E_{\hat{y} \sim p(\hat{y}|x; \varphi)} [\log p_{\text{dec}}(\hat{x}|\hat{y}; \theta)]. \quad (9)$$

To calculate Eq. (9), we need to get  $p(\hat{y}|x; \varphi)$  and  $p_{\text{dec}}(\hat{x}|\hat{y}; \theta)$  first. For the JSCC system, there exists a Markov chain,  $x \rightarrow y \rightarrow \hat{y} \rightarrow \hat{x}$ . Thus the joint probability  $p(x, \hat{x}, y, \hat{y})$  can be modelled as,

$$p(x, \hat{x}, y, \hat{y}) = p(x) p_{\text{enc}}(y|x; \varphi) p_{\text{channel}}(\hat{y}|y; \varepsilon) p_{\text{dec}}(\hat{x}|\hat{y}; \theta), \quad (10)$$

where  $\varepsilon$  is the error probability of channel. Then, we have

$$p(\hat{y}|x; \varphi) = \sum_{y \in \mathcal{Y}} p_{\text{enc}}(y|x; \varphi) p_{\text{channel}}(\hat{y}|y; \varepsilon). \quad (11)$$

Similar to<sup>14</sup> and<sup>15</sup>,  $y$  follows multi-dimensional Bernoulli distribution and its bits are independent of each other. The outputs of the encoder neural network are treated as the parameters of this Bernoulli distribution. Let  $f_{\varphi}(\cdot)$  represent the function of encoder neural network. The bits in  $y$  obey Bernoulli distribution with parameters  $f_{\varphi}(x)$ . The conditional probability of the encoder is

$$p_{\text{enc}}(y|x; \varphi) = \prod_{m=1}^M (f_{\varphi}(x))^{y_m} (1 - f_{\varphi}(x))^{1-y_m} \quad (12)$$

where  $M$  represents the length of  $y$ , i.e., the number of transmitted bits, and  $y_m$  represents the  $m$ -th bit of  $y$ . For the binary symmetric channel (BSC)<sup>14,15</sup>, each bit of  $y$  is independently flipped ( $1 \rightarrow 0$  or  $0 \rightarrow 1$ ) with probability  $\varepsilon$ . The channel transition probability can be formulated as,

$$p_{\text{BSC}}(\hat{y}|y; \varepsilon) = \prod_{m=1}^M \varepsilon^{y_m \oplus \hat{y}_m} (1 - \varepsilon)^{y_m \oplus \hat{y}_m \oplus 1}, \quad (13)$$

where  $\oplus$  denotes modulo-2 addition. Similar to<sup>14</sup>, the whole encoding distribution is formulated as,

$$p(\hat{y}|x; \varphi) = \prod_{m=1}^M (f_{\varphi}(x) - 2f_{\varphi}(x)\varepsilon + \varepsilon)^{\hat{y}_m} (1 - (f_{\varphi}(x) - 2f_{\varphi}(x)\varepsilon + \varepsilon))^{1-\hat{y}_m}, \quad (14)$$

which follows Bernoulli distribution with parameter  $(f_\varphi(x) - 2f_\varphi(x)\varepsilon + \varepsilon)$ .

In this work, reconstruction  $\hat{x}$  is probabilistic and parameterized by the decoder neural network  $g_\theta(\cdot)$ . Each pixel of  $\hat{x}$  is modelled as independent Gaussian distribution and the parameters of Gaussian distribution are the outputs of decoder. Thus, for  $p_{\text{dec}}(\hat{x}|\hat{y}; \theta)$ , we have

$$p_{\text{dec}}(\hat{x}|\hat{y}; \theta) \sim N(g_\theta(\hat{y}), I) \quad (15)$$

where  $N$  represents the Gaussian distribution. We assume that  $p_{\text{data}}(x) = \frac{1}{N}$  and the tractable lower bound of  $I(x, \hat{y})$  can be calculated by introducing Eq. (15) and Eq. (14) into Eq. (9).

Next, we derive the applicable form of  $I(x, y)$  in the considered system. Instead of minimizing  $I(x, y)$ , we minimize its upper bound. Since we make no assumption on the distribution of  $y$ , the popular variational upper bound (VUB)<sup>18</sup>,  $KL(p(y|x) | r(y))$ , cannot be used, where  $r(y)$  is an approximation of  $p(y)$ . Instead, we exploit another upper bound of mutual information called CLUB<sup>26</sup>,

$$I(x, y) \leq I_{\text{CLUB}}(x, y) = E_{p(x, y)} [\log p(y|x)] - E_{p(x)} E_{p(y)} [\log p(y|x)]. \quad (16)$$

$I_{\text{CLUB}}(x, y)$  can be calculated by the Monte Carlo method as,

$$I_{\text{CLUB}}(x, y) \approx \left( \frac{1}{N} \sum_{i=1}^N \log p_{\text{enc}}(y_i|x_i; \varphi) - \frac{1}{N^2} \sum_{i=1}^N \sum_{j=1}^N \log p_{\text{enc}}(y_j|x_i; \varphi) \right), \quad (17)$$

where  $N$  is the number of sample pairs  $\{x_i, y_i\}$ . Since  $p_{\text{enc}}(y|x; \varphi)$  is the probability of Bernoulli distribution, Eq. (17) is tractable and differentiable. Thus, instead of minimizing the true value, we minimize the estimated upper bound of  $I(x, y)$  in Eq. (17). Overall, by replacing  $I(x, \hat{y})$  and  $I(x, y)$  in Eq. (7) by Eq. (9) and Eq. (17), respectively, we can optimize the IB objective.

---

#### Algorithm 1 AIB-JSCC

---

**Input:** Dataset(X) to be compressed; channel error probability  $\varepsilon$ ; Coefficients  $k_p$ ,  $k_i$  and  $k_d$ ;

Minimal value of hyperparameter  $\beta : \beta_{\min}$ .

**Output:** Learned JSCC encoder  $p_{\text{enc}}(y|x; \varphi)$  and decoder  $p_{\text{dec}}(x|\hat{y}; \theta)$

Initialize the parameters of encoder  $p_{\text{enc}}(y|x; \varphi)$ , the parameter of decoder  $p_{\text{dec}}(x|\hat{y}; \theta)$ ,  $I[0] = 0$ ,  $i = 1$ , hyperparameter  $\beta = \beta_{\min}$ .

**while** not converge **do**

    Sample a batch of samples from Dataset:  $x \sim p_{\text{data}}(x)$ ;

    Sample the corresponding latent codes  $y \sim p_{\text{enc}}(y|x; \varphi)$ ;

    Sample the corresponding noisy latent codes  $\hat{y} \sim p(\hat{y}|x; \varphi)$ ;

    Update  $\varphi$  according to the objective in Eq. (29):  $\max_{\varphi} L_{\text{rec}}(\varphi, \theta; x, \varepsilon) - \beta L_{\text{com}}(\varphi; x)$

    Update  $\theta$  according to:  $\max_{\theta} L_{\text{rec}}(\varphi, \theta; x, \varepsilon)$

**if** an epoch of training finishes **then**

    Calculate MSE[i] according to Eq. (28),  $\beta_{\max}[i]$  according to Eq. (25);

$P[i] \leftarrow K_p \text{MSE}[i]$

$I[i] \leftarrow I[i-1] + K_i \text{MSE}[i]$

$D[i] \leftarrow K_d (\text{MSE}[i] - \text{MSE}[i-1])$

**if**  $\beta_{\min}[i] < \beta[i] < \beta_{\max}[i]$  **then**

$\beta[i+1] \leftarrow \beta_{\max}[i] + P[i] - I[i] - D[i]$ ;

**end if**

**if**  $\beta_{\max}[i] < \beta[i]$  **then**

$\beta[i+1] \leftarrow \beta_{\max}[i]$

**end if**

**if**  $\beta[i] < \beta_{\min}[i]$  **then**

$\beta[i+1] \leftarrow \beta_{\min}[i]$

**end if**

$i \leftarrow i+1$

**end if**

**end while**

---

### Adaptive IB algorithm

In our proposed IB objective, the value of  $\beta$  controls the trade-off between the compression level and the reconstruction quality. Therefore, it is significant to propose a suitable algorithm to determine  $\beta$ . In particular, if  $\beta$  is large, the term  $I(x, y)$  will dominate the loss function and  $y$  will aggressively discard information of  $x$ . However, if  $\beta$  is excessively large, the global optimal encoder distribution may be  $p(y|x) = p(y)$ , which means  $y$  is independent of  $x$ . In this case,  $y$  and  $\hat{y}$  contain no information about  $x$ , i.e.  $I(x, \hat{y}) = I(x, y) = 0$ , and thus reconstructing  $x$  from  $\hat{y}$  becomes infeasible. Therefore, it is necessary to limit  $\beta$  below an upper bound to ensure that  $x$  and  $y$  are dependent. The sufficient condition for  $x$  and  $y$  being dependent is<sup>27</sup>

$$\begin{aligned} \beta &\leq \beta_{\max}[w] = \frac{I(x, \hat{y})}{I(x, y)} \\ \text{subject to : } &x \rightarrow y \rightarrow \hat{y} \end{aligned} \quad (18)$$

At the end of each epoch,  $I(x, \hat{y})$  and  $I(x, y)$  are fixed since networks are fixed, and thus we can estimate  $I(x, \hat{y})$  and  $I(x, y)$  according to  $I(x, \hat{y}) = H(\hat{y}) - H(\hat{y}|x)$ , and  $I(x, y) = H(y) - H(y|x)$ . We estimate  $H(y)$  and  $H(y|x)$  separately. To get  $H(y)$ , we estimate  $p(y_m)$  by,

$$p(y_m) \approx \frac{1}{N} \sum_{i=1}^N p(y_m|x_i). \quad (19)$$

Since the bits in codewords are assumed to be independent, the entropy of  $y$  is equal to the sum of the entropies of all bits,

$$H(y) = \sum_{m=1}^M H(y_m) \approx \sum_{m=1}^M -\log \left( \frac{1}{N} \sum_{i=1}^N p(y_m|x_i) \right). \quad (20)$$

To calculate  $H(y|x)$ , we assume  $p(x) = \frac{1}{N}$ , and thus,

$$H(y|x) = \frac{1}{N} \sum_{i=1}^N H(p(y|x_i)). \quad (21)$$

Since the bits are independent, we have

$$H(y|x) = \frac{1}{N} \sum_{m=1}^M \sum_{i=1}^N H(p(y_m|x_i)) \approx \frac{1}{N} \sum_{m=1}^M \sum_{i=1}^N -\log(p(y_m|x_i)). \quad (22)$$

Therefore, since  $I(x, y) = H(y) - H(y|x)$ , we can estimate  $I(x, y)$  by

$$I(x, y) \approx I_e(x, y) = \frac{1}{N} \sum_{m=1}^M \sum_{i=1}^N \log(p(y_m|x_i)) - \sum_{m=1}^M \frac{1}{N} \log \left( \sum_{i=1}^N p(y_m|x_i) \right). \quad (23)$$

Similar to Eq. (20) and Eq. (22),  $H(\hat{y}) \approx \frac{1}{N} \sum_{m=1}^M \sum_{i=1}^N \log(p(\hat{y}_m|x_i))$  and  $H(\hat{y}|x) \approx \sum_{m=1}^M \frac{1}{N} \log \left( \sum_{i=1}^N p(\hat{y}_m|x_i) \right)$ . We can estimate  $I(x, \hat{y})$  as,

$$I(x, \hat{y}) \approx I_e(x, \hat{y}) = \frac{1}{N} \sum_{m=1}^M \sum_{i=1}^N \log(p(\hat{y}_m|x_i)) - \sum_{m=1}^M \frac{1}{N} \log \left( \sum_{i=1}^N p(\hat{y}_m|x_i) \right). \quad (24)$$

Then  $\beta_{\max}$  at the  $w$ -th epoch can be approximated as,

$$\beta_{\max}[w] = \frac{I_e(x, \hat{y}; w)}{I_e(x, y; w)}, \quad (25)$$

where  $I_e(x, \hat{y}; w)$  and  $I_e(x, y; w)$  represent  $I_e(x, \hat{y})$  and  $I_e(x, y)$  at the  $w$ -th epoch, respectively.

From Eq. (7), as  $\beta$  increases, the mutual information between  $x$  and  $y$  decreases. At the beginning,  $y$  contains abundant redundancy due to imperfect map from the source information to the transmitted codewords. Therefore, in the initial stages, we must set a relatively large  $\beta$  to squeeze more redundant information in  $y$ . As the training processes, the value of  $\beta$  should decrease since the corresponding redundancy information in  $y$  gradually decreases. The value of  $\beta$  will finally converge to a constant, when the proposed IB-JSCC achieves the optimal trade-off between the reconstruction quality and the compression

ratio. To determine the value of  $\beta$  in each epoch, IB-JSCC introduces a PID control algorithm, which analyzes the past errors and predicts the future errors to determine the current value of  $\beta$ . The discrete form of PID controller can be expressed as<sup>28</sup>,

$$\beta [w] = K_p e [w] - K_i \sum_{k=0}^{w-1} e [k] - K_d (e [w] - e [w - 1]), \quad (26)$$

where  $\beta [w]$  is the output of the controller at time  $w$ ,  $K_p$  is the proportional gain,  $K_i$  is the integral gain,  $K_d$  is the differential gain, and error  $e [w]$  is the difference between the actual value and the desired value at time  $w$ . In addition,  $K_p e [w]$  is the proportional (P) term, which can respond to the change of error quickly and provide a global control proportional to the error;  $K_i \sum_{k=0}^{w-1}$  is the integral (I) term, which continues to increase as long as the error is greater than 0 and can eliminate steady-state errors;  $K_d (e [w] - e [w - 1])$  is the differential (D) term, which can reduce the overshoot and improve the system's stability and transient response<sup>28</sup>. The PID controller continuously calculates error  $e [w]$  and the weighted sum of these three terms, and then applies a correction on the system to reduce the error  $e [w]$ . We employ Eq. (26) to adjust  $\beta$  at the end of each epoch. Since the goal of introducing Eq. (26) is tuning  $\beta$  so as to balance the ability of reconstruction and compression and MSE should be 0 if the balance is perfect, we treat MSE between the original image,  $x$ , and the reconstructed image,  $\hat{x}$ , at the  $w$ -th epoch as  $e [w]$ . Then  $\beta$  will change in the direction to reduce MSE. To guarantee that the compression ratio is smaller than the maximal compression ratio bounded by the IB principle, we add  $\beta_{\max} [w]$  to constrain the range of  $\beta$  and let  $\beta$  gradually decrease from its upper bound as the training processes. The proposed formula of  $\beta$  at the  $w$ -th epoch is

$$\beta [w] = \beta_{\max} [w] + K_p \text{MSE} [w] - K_i \sum_{k=0}^{w-1} \text{MSE} [k] - K_d (\text{MSE} [w] - \text{MSE} [w - 1]), \quad (27)$$

and

$$\text{MSE} [k] = \frac{1}{N} \sum_{i=1}^N (x_i - \hat{x}_i [k])^2 \quad (28)$$

where  $\hat{x}_i [k]$  is the recovered image of  $x_i$  at the  $k$ -th epoch. At the end of each epoch,  $\beta$  changes according to Eq. (27). We can adjust  $K_p$ ,  $K_i$  and  $K_d$  to obtain proper  $\beta$ . New  $\beta$  is then used in the loss function of the next epoch. The whole training procedure of the proposed AIB-JSCC that combines the proposed IB objective and the adaptive IB algorithm is summarized in Algorithm 1.

## Experiments

In this section, we first introduce the optimization procedure of the AIB-JSCC system. Then, to validate our proposed schemes, we compare the reconstruction and compression capabilities of the traditional SSCC, our proposed schemes, and the state-of-the-art JSCC method. There are two existing works on JSCC with discrete channels for image transmission: NECST<sup>14</sup> and IABF<sup>15</sup>. Since IABF has been proved to have better performance than NECST, we choose IABF as state-of-the-art JSCC method and compare its performance with the proposed AIB-JSCC. Finally, we assess the quality of the codewords extracted by different methods and demonstrate that the codewords extracted by AIB-JSCC are semantic and robust to noise. The experiments are carried on the following datasets: MNIST<sup>29</sup>, Omniglot<sup>30</sup>, CIFAR10<sup>31</sup>, Street View Housing Numbers tsicon (SVHN)<sup>32</sup> and CelebA<sup>33</sup> to account for different image sizes and colors. To make a fair comparison, the networks and settings used in our proposed schemes are same with those used in IABF.

### Optimization Procedure

Here, we further rewrite the loss function in Eq. (7) as,

$$\max_{\varphi, \theta} L_{\text{rec}} (\varphi, \theta; x, \varepsilon) - \beta L_{\text{com}} (\varphi; x), \quad (29)$$

where  $L_{\text{rec}}$  represents  $I(x, \hat{y})$ , and  $L_{\text{com}}$  represents  $I(x, y)$ . Equation (29) is used as the loss function to train the end-to-end encoder and decoder neural network. The optimization of the parameters of encoder,  $\varphi$ , is related to both  $L_{\text{rec}}$  and  $L_{\text{com}}$ . However, the optimization of the parameters of decoder,  $\theta$ , is only related to  $L_{\text{rec}}$ , which means the compression of mutual information is irrelevant to the decoder. Therefore, we optimize the encoder and the decoder alternately. In addition,  $L_{\text{rec}}$  is non-differentiable in its current form. Since the channel is discrete, the gradient of  $L_{\text{rec}}$  with respect to the encoder parameters,  $\varphi$ ,

is non-trivial. Following IABF, we utilize VIMCO<sup>34</sup>, a multi-sample variational lower bound objective, to obtain a low-variance estimation of gradients. Therefore, the adopted form of  $L_{\text{rec}}$  is

$$L_{\text{rec}}(\varphi, \theta; x, \varepsilon) = \sum_{x \in D} E_{y^{1:K} \sim p(y|x; \varepsilon, \varphi)} \left[ \log \frac{1}{K} \sum_{i=1}^K p_{\text{dec}}(x|y^i; \theta) \right], \quad (30)$$

where  $K = 5$  is the number of multi-sample used in VIMCO.

## Reconstruction results

Datasets	Methods	MSE under different error probabilities			
		0.1	0.2	0.3	0.4
100-bit MNIST	IABF	13.251	22.026	33.176	46.555
	IB-JSCC	13.012	20.983	33.128	45.03
	AIB-JSCC	<b>12.902</b>	<b>20.784</b>	<b>33.105</b>	<b>45.027</b>
200-bit Omniglot	IABF	24.132	31.373	38.936	47.608
	IB-JSCC	23.896	31.101	38.932	47.141
	AIB-JSCC	<b>23.89</b>	<b>31.092</b>	<b>38.868</b>	<b>47.14</b>
500-bit CIFAR10	IABF	55.351	70.525	83.193	116.281
	IB-JSCC	55.177	65.987	80.941	115.532
	AIB-JSCC	<b>54.464</b>	<b>64.969</b>	<b>80.642</b>	<b>114.615</b>

**Table 1.** MSE of IABF vs. IB-JSCC vs. AIB-JSCC.

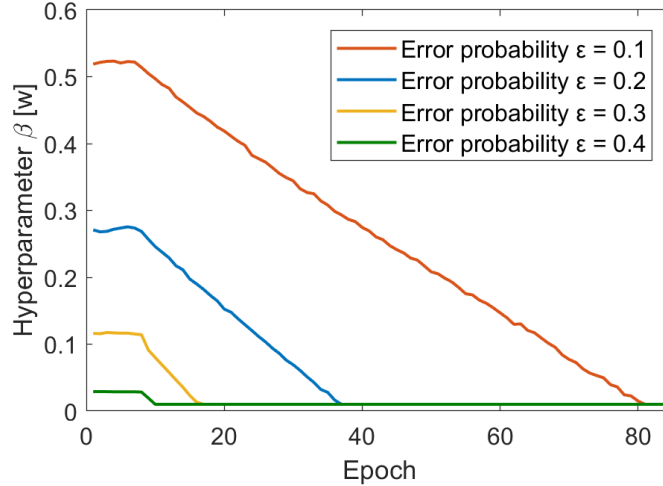


**Figure 2.** The value of hyperparameter  $\beta [w]$  with respect to training epoch.

### Error correction

This experiment compares the error correction performance of IABF, IB-JSCC, and AIB-JSCC, where IB-JSCC stands for the JSCC system simply applying our proposed IB objective without adaptive IB algorithm. Similar to IABF, we fix the lengths of codeword used in IB-JSCC and AIB-JSCC. We compare IB-JSCC and AIB-JSCC on three datasets, MNIST, Omniglot and CIFAR10. The lengths of codeword for IB-JSCC and AIB-JSCC are 100, 200, and 500, respectively.  $K_p$  and  $K_d$  are all set to be 0.001, and  $K_i$  is chosen from  $\{0.001, 0.0001\}$ .  $\beta_{\min}$  is chosen from  $\{0.01, 0.001\}$ . We store the model with the lowest MSE on valid set during training. Then, for different datasets and error probabilities, we present the corresponding distortions (reconstruction errors) of the model on the test sets in Table 1. As shown in Table 1, IB-JSCC always outperforms IABF on all three datasets and error probabilities. Besides, AIB-JSCC can further decrease the distortion on the basis of IB-JSCC, which

validates the effectiveness of the proposed adaptive IB algorithm. In particular, IB-JSCC and AIB-JSCC can reduce MSE more on the RGB dataset CIFAR10 than on the greyscale dataset MNIST and Omniglot, which implies that, IB-JSCC and AIB-JSCC can extract information more precisely and recover complex images better.

In Figure 2, we further present the trend of AIB-JSCC’s hyperparameter  $\beta [w]$  with respect to training epoch on CIFAR10 dataset under different error probabilities. We can observe that as we expect,  $\beta [w]$  gradually decreases when training processes. In addition, when error probability gets large, the noisy codewords need to preserve more information of input  $I(x, \hat{y})$  to resist the noise interference. Therefore, as shown in Figure 2, the value of  $\beta [w]$  reduces as the error probability increases, which can prevent from losing useful information on  $I(x, \hat{y})$ .



**Figure 3.** Visual comparison between AIB-JSCC and IABF for the sample images of the SVHN dataset.

We also compare the visual reconstruction results of AIB-JSCC and IABF. The experiment is carried on the SVHN dataset. The systems are trained and tested when error probability  $\epsilon=0.1$ , and the length of codeword is 500. The recovered images of IABF and AIB-JSCC for the sample images from SVHN test dataset are shown in Figure 3. We can observe that the images recovered by AIB-JSCC are closer to the original images than those recovered by IABF. Moreover, we can distinguish the numbers in the images recovered by AIB-JSCC more easily than IABF, which demonstrates that AIB-JSCC can preserve more semantic information in the recovered images.

Datasets	Methods	Number of network parameters ( $\times 10^5$ )	Inference time per image (ms)
100-bit MNIST	IABF	11.86	0.4
	AIB-JSCC	<b>11.345</b>	0.4
200-bit Omniglot	IABF	13.36	0.743
	AIB-JSCC	<b>12.345</b>	<b>0.372</b>
500-bit CIFAR10	IABF	5.679	1
	AIB-JSCC	<b>3.164</b>	<b>0.8</b>

**Table 2.** The number of network parameters and the inference time of IABF and AIB-JSCC.

### Complexity and convergence

We compare the complexity of IABF and AIB-JSCC by calculating the number of encoder and decoder network parameters and the inference time. The corresponding results are present in Table 2. We can observe that AIB-JSCC has fewer parameters and needs less inference time, which means AIB-JSCC has lower computational complexity than IABF. We also compare the performance of convergence by comparing the validation reconstruction MSE. Figure 4 shows the changes of validation reconstruction MSE with respect to training time steps for IABF and AIB-JSCC. We can observe that the trend of IABF and AIB-JSCC is similar when error probability  $\epsilon$  is 0.1, 0.2. When error probability gets larger, AIB-JSCC converges more stably than IABF. When  $\epsilon$  is 0.4, there is severe overfitting in IABF while AIB-JSCC still converges stably.

### Downstream classification

We perform the classification on the recovered images to demonstrate that the images reconstructed by AIB-JSCC contain abundant information for downstream tasks. We first train 4 different classifiers, multilayer perceptron (MLP), support vector machines (SVM), decision trees (DT), random forests (RF), with the raw MNIST dataset, and then test the trained classifiers

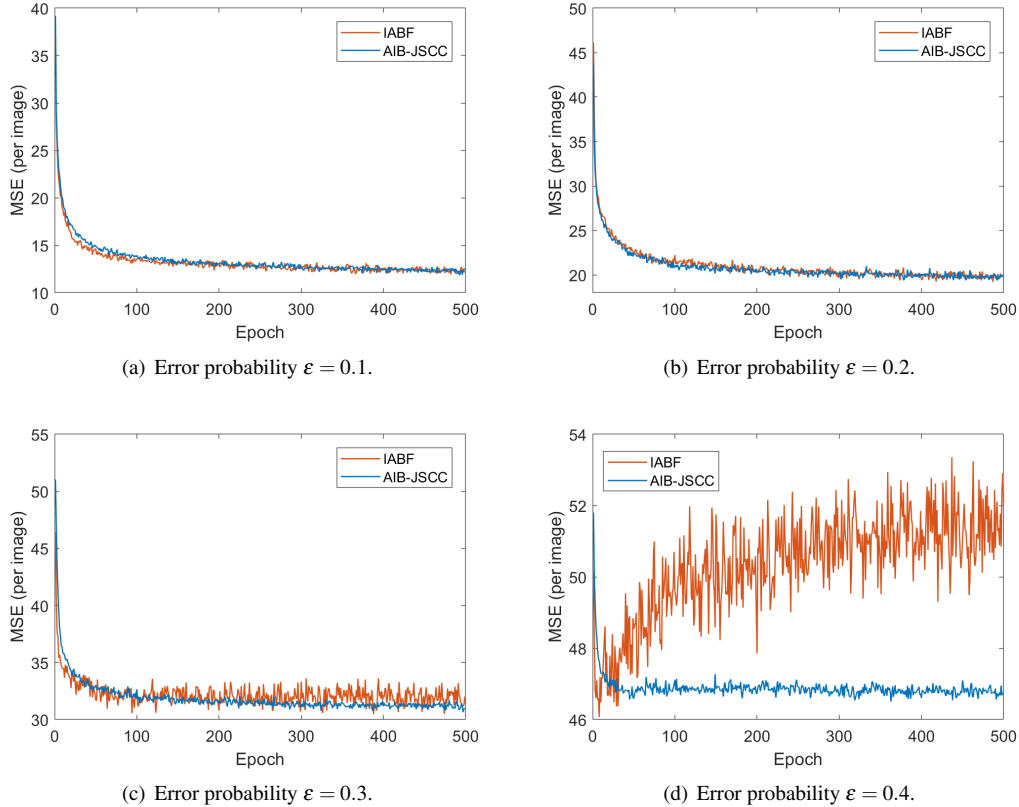


**Figure 4.** The reconstruction MSE (per image) of IABF and AIB-JSCC on MNIST dataset. The error is calculated on validation set during training.

with the images recovered by AIB-JSCC and IABF from the MNIST test set. Table 3 shows the classification accuracy of IABF and AIB-JSCC with respect to different error probabilities. From the table, the classification accuracy of the images recovered by AIB-JSCC is always higher than IABF over different error probabilities, which illustrates that the images recovered by AIB-JSCC can preserve more semantic information.

## Compression results

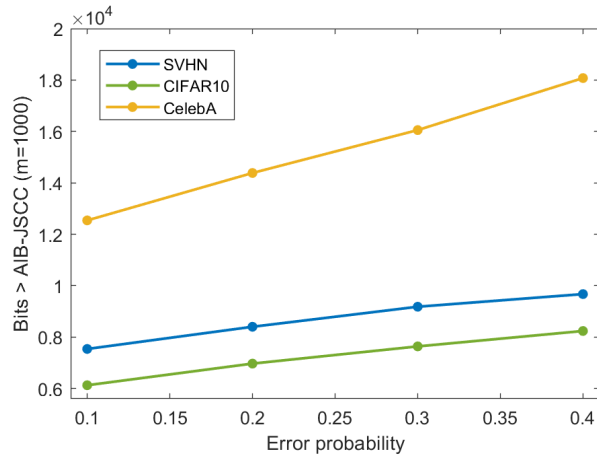
### Comparison with SSCC

This experiment compares the compression performance of AIB-JSCC and traditional SSCC. In AIB-JSCC, we still fix the length of codeword  $M$  and calculate the average MSE of the trained model on test set as distortion. For traditional SSCC, we use the JPEG as the source coding, and we assume the channel coding is ideal. Let  $d_\epsilon$  denote the reconstruction error of an image recovered by AIB-JSCC when error probability is  $\epsilon$ . Then we encode this image at distortion level  $d_\epsilon$  with JPEG encoder and obtain the number of bits  $f(d_\epsilon)$  used by JPEG encoder. For the BSC channel with error probability  $\epsilon$ , the channel capacity is  $C = 1 - H_b(\epsilon)$ , where  $H_b(\cdot)$  denotes the binary entropy function. According to information theory, if the channel capacity is  $C$ , the minimal number of bits (channel usages) required to correctly transmit  $f(d_\epsilon)$  bits over the channel is  $\frac{f(d_\epsilon)}{C}$ . Therefore, we estimate the number of bits used by SSCC as  $\frac{f(d_\epsilon)}{1 - H_b(\epsilon)}$ . Note that  $\frac{f(d_\epsilon)}{1 - H_b(\epsilon)}$  is achievable only in the ideal scenario where the length of codeword is infinite. However, in the practical scenario, the required transmitted bits (channel usages) will be much more.

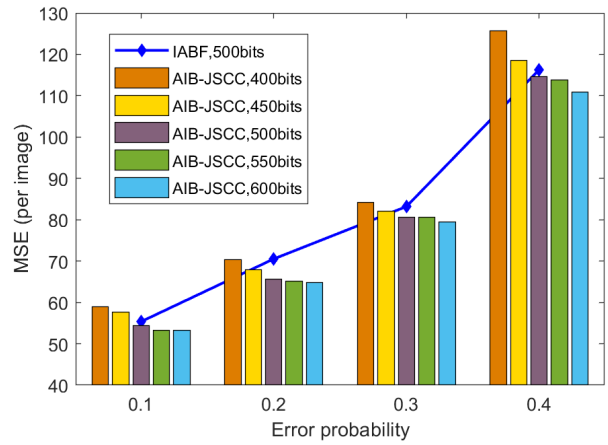
We conduct AIB-JSCC and JPEG encoding on three RGB datasets: SVNH, CIFAR10, CelebA. In AIB-JSCC, the lengths of codeword used on SVNH, CIFAR10, and CelebA are 500, 500, and 1000, respectively. We compute  $\frac{f(d_\epsilon)}{1 - H_b(\epsilon)}$  for each image and obtain the average across the test set as the number of bits that SSCC needs on these datasets. The additional number of bits needed by SSCC are illustrated in Figure 5 (a). From the figure, JPEG + ideal channel coding needs much more bits at all datasets and error probabilities in order to achieve the same reconstruction error. As the error probability  $\epsilon$  increases, the additional required number of bits (channel usages) will increase. In particular, AIB-JSCC only needs around 5% bits that JPEG + ideal channel coding needs when  $\epsilon = 0.4$ .

Classifiers	Methods	Acc under different error probabilities			
		0.1	0.2	0.3	0.4
MLP	IABF	0.932	0.817	0.637	0.3311
	AIB-JSCC	<b>0.937</b>	<b>0.8813</b>	<b>0.692</b>	<b>0.386</b>
SVM	IABF	0.932	0.821	0.619	0.312
	AIB-JSCC	<b>0.935</b>	<b>0.884</b>	<b>0.694</b>	<b>0.358</b>
DT	IABF	0.51	0.391	0.297	0.177
	AIB-JSCC	<b>0.537</b>	<b>0.469</b>	<b>0.337</b>	<b>0.2</b>
RF	IABF	0.673	0.522	0.288	0.176
	AIB-JSCC	<b>0.708</b>	<b>0.549</b>	<b>0.308</b>	<b>0.181</b>

**Table 3.** Classification accuracy of the images recovered by IABF and AIB-JSCC.



(a) The additional number of bits that JPEG + Ideal channel coding needs.



(b) MSE (per image) of IABF and AIB-JSCC.

**Figure 5.** The performance on compression of SSCC, IABF and AIB-JSCC. (a) The additional number of bits that JPEG + Ideal channel coding needs than AIB-JSCC. (b) MSE (per image) of IABF and AIB-JSCC on CIFAR10 test dataset.

### Comparison with the state-of-the-art JSCC scheme

We also compare the compression performance of AIB-JSCC and IABF. We vary the lengths of codeword used in AIB-JSCC from 400 to 600 and repeat the experiments on CIFAR10 with various error probabilities. The corresponding distortions are plotted in Figure 5 (b). From the figure, when the length of codeword increases, MSE of AIB-JSCC gradually decreases and the trend that MSE changes with the length of codeword are similar under different error probabilities of the BSC. In addition, when  $\varepsilon = 0.1, 0.3, 0.4$ , AIB-JSCC requires 15, 70, 20 less bits than IABF, respectively. When  $\varepsilon = 0.2$ , AIB-JSCC can reduce more than 100 bits, i.e., 20% than IABF.

### Quality of codewords

We further evaluate the learned codewords by observing its semantic preservation and information redundancy. We first train the AIB-JSCC system with error probability  $\varepsilon = 0.1$ . Then, we can obtain the learned 100-bit codewords extracted from randomly selected 5k images in the MNIST test dataset. Finally, we inject test noise into codewords and obtain the noisy codewords when test error probability  $\varepsilon_{\text{test}} = 0.1, 0.2, 0.3, 0.4$ , respectively. To visualize and assess the codewords, we utilize t-Distributed Stochastic Neighbor Embedding (t-SNE)<sup>35</sup> to project the codewords into a 2-dimensional space. We conduct t-SNE on the parameters of the 4 groups of noisy codewords and plot the corresponding points in Figure 6. Each color represents a number, i.e. a type in MNIST dataset. From the figure, noisy codewords having the same color are close to each other and well separated with other colors. This means the test dataset is well classified. Besides, the distributions of codewords are similar under different  $\varepsilon_{\text{test}}$ , which means the codewords can resist noise and preserve semantic information. Overall, the codewords extracted by AIB-JSCC are semantic and robust to noise.

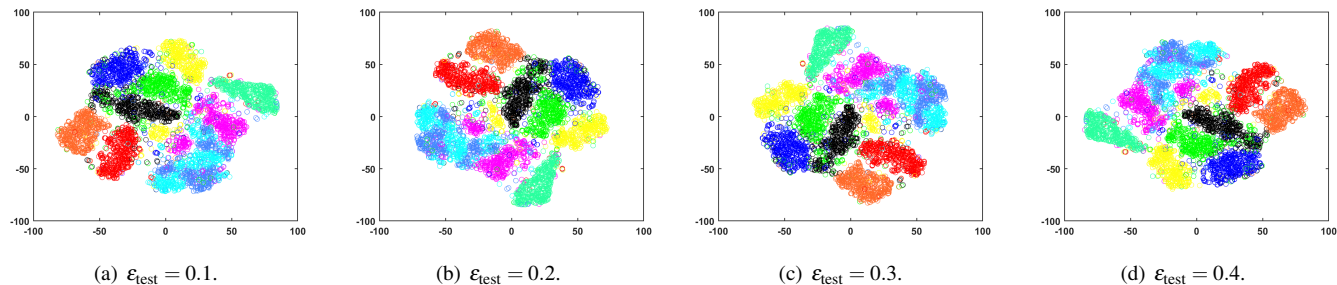


**Figure 6.** t-SNE visualization of codewords extracted by AIB-JSCC for test set of MNIST dataset. The network is trained with error probability  $\varepsilon = 0.1$  and tested with different test error probabilities  $\varepsilon_{\text{test}}$ . Each color represents a different class.

## Discussion

In this work, we propose an AIB-JSCC scheme, which can adaptively minimize the rate and distortion at the same time to achieve better reconstruction quality, larger compression ratio, and lower computational complexity than the state-of-the-art approaches. Specifically, we first derived a mathematically tractable form of IB objective for the JSCC system. To promise the dependency between the codewords and input, we derived the closed-form upper bound for hyperparameter  $\beta$  of the loss function. We further proposed an algorithm which can adaptively adjust  $\beta$ . Experiments results have shown that with fixed length of codeword, IB-JSCC always achieved lower reconstruction error than IABF over various error probabilities and datasets. AIB-JSCC can further decrease the reconstruction error of IB-JSCC, which demonstrated the effectiveness of the proposed adaptive IB algorithm. In addition, the images recovered by AIB-JSCC have better visual performance and obtain higher accuracy on downstream classification task than IABF. AIB-JSCC also has lower computational complexity than IABF. For a given reconstruction error, AIB-JSCC always permitted larger compression ratio than SSCC and IABF. In particular, AIB-JSCC only needed around 5% and 80% bits compared with SSCC and IABF. Moreover, the codewords extracted by AIB-JSCC were robust to noise. The overall results showed that the proposed schemes can significantly reduce the required amount of the transmitted data, and improve the reconstruction quality and downstream tasks accuracy with lower computational complexity. In the future, we will further investigate IB guided JSCC systems for analog channels.

## References

1. Shannon, C. E. A mathematical theory of communication. *Bell Syst. Technol. J.* **27**, 379–423 (1948).
2. Berlekamp, E., McEliece, R. & Van Tilborg, H. On the inherent intractability of certain coding problems (corresp.). *IEEE Trans. Inf. Theory* **24**, 384–386 (1978).
3. Yang, P., Xiao, Y., Xiao, M. & Li, S. 6g wireless communications: Vision and potential techniques. *IEEE Netw.* **33**, 70–75 (2019).
4. Letaief, K. B., Chen, W., Shi, Y., Zhang, J. & Zhang, Y.-J. A. The roadmap to 6g: Ai empowered wireless networks. *IEEE Commun. Mag.* **57**, 84–90 (2019).
5. Gallager, R. G. *Information theory and reliable communication*, vol. 2 (Springer, 1968).
6. Gastpar, M., Rimoldi, B. & Vetterli, M. To code, or not to code: Lossy source-channel communication revisited. *IEEE Trans. Inf. Theory* **49**, 1147–1158 (2003).
7. Cheung, G. & Zakhor, A. Bit allocation for joint source/channel coding of scalable video. *IEEE Trans. Image Process.* **9**, 340–356 (2000).
8. Heinen, S. & Vary, P. Transactions papers source-optimized channel coding for digital transmission channels. *IEEE Trans. Commun.* **53**, 592–600 (2005).
9. Boursoulatz, E., Kurka, D. B. & Gündüz, D. Deep joint source-channel coding for wireless image transmission. *IEEE Trans. Cogn. Commun. Netw.* **5**, 567–579 (2019).
10. Kurka, D. B. & Gündüz, D. Deepjssc-f: Deep joint source-channel coding of images with feedback. *IEEE J. Sel. Areas Inf. Theory* **1**, 178–193 (2020).
11. Xu, J. *et al.* Wireless image transmission using deep source channel coding with attention modules. *IEEE Trans. Circuits Syst. Video Technol.* (2021).

12. Wallace, G. K. The jpeg still picture compression standard. *IEEE Trans. Consum. Electron.* **38**, xviii–xxxiv (1992).
13. Skodras, A., Christopoulos, C. & Ebrahimi, T. The jpeg 2000 still image compression standard. *IEEE Signal Process. Mag.* **18**, 36–58 (2001).
14. Choi, K., Tatwawadi, K., Grover, A., Weissman, T. & Ermon, S. Neural joint source-channel coding. In *Int. Conf. Mach. and Learn.*, 1182–1192 (2019).
15. Song, Y. *et al.* Infomax neural joint source-channel coding via adversarial bit flip. In *Proc. AAAI Conf. Artificial Intell.*, vol. 34, 5834–5841 (2020).
16. Chen, X. *et al.* Infogan: Interpretable representation learning by information maximizing generative adversarial nets. In *Adv. Neural Inf. Process. Syst.*, 2180–2188 (2016).
17. Tishby, N., Pereira, F. C. & Bialek, W. The information bottleneck method. *arXiv preprint physics/0004057* (2000).
18. Alemi, A. A., Fischer, I., Dillon, J. V. & Murphy, K. Deep variational information bottleneck. *arXiv preprint arXiv:1612.00410* (2016).
19. Belinkov, Y., Henderson, J. *et al.* Variational information bottleneck for effective low-resource fine-tuning. In *Int. Conf. Learn. Repr.* (2020).
20. Du, Y. *et al.* Learning to learn with variational information bottleneck for domain generalization. In *European Conf. Comput. Vision*, 200–216 (2020).
21. Tishby, N. & Zaslavsky, N. Deep learning and the information bottleneck principle. In *IEEE Inf. Theory Workshop (ITW)* (2015).
22. Lee, J., Choi, J., Mok, J. & Yoon, S. Reducing information bottleneck for weakly supervised semantic segmentation. In *Adv. Neural Inf. Process. Syst.*, vol. 34 (2021).
23. Goldfeld, Z. & Polyanskiy, Y. The information bottleneck problem and its applications in machine learning. *IEEE J. Sel. Areas Inf. Theory* **1**, 19–38 (2020).
24. Amjad, R. A. & Geiger, B. C. Learning representations for neural network-based classification using the information bottleneck principle. *IEEE Trans. Pattern Anal. Mach. Intell.* **42**, 2225–2239 (2019).
25. Qian, W., Chen, B., Zhang, Y., Wen, G. & Gechter, F. Multi-task variational information bottleneck. *arXiv preprint arXiv:2007.00339* (2020).
26. Cheng, P. *et al.* Club: A contrastive log-ratio upper bound of mutual information. In *Int. Conf. Mach. and Learn.*, 1779–1788 (2020).
27. Wu, T., Fischer, I., Chuang, I. L. & Tegmark, M. Learnability for the information bottleneck. In *Uncertainty in Artificial Intell.*, 1050–1060 (2020).
28. Li, Y. *et al.* Learning disentangled user representation based on controllable vae for recommendation. In *Int. Conf. Database Syst. Advanced Applicat.*, 179–194 (2021).
29. LeCun, Y. The mnist database of handwritten digits. <http://yann.lecun.com/exdb/mnist/> (1998).
30. Lake, B. M., Salakhutdinov, R. & Tenenbaum, J. B. Human-level concept learning through probabilistic program induction. *Science* **350**, 1332–1338 (2015).
31. Krizhevsky, A. & Hinton, G. Learning multiple layers of features from tiny images. *Handb. Syst. Autoimmune Dis.* **1** (2009).
32. Netzer, Y. *et al.* Reading digits in natural images with unsupervised feature learning. In *Adv. Neural Inf. Process. Syst. Workshop* (2011).
33. Liu, Z., Luo, P., Wang, X. & Tang, X. Deep learning face attributes in the wild. In *Proc. IEEE Int. Conf. Comput. Vision*, 3730–3738 (2015).
34. Mnih, A. & Rezende, D. Variational inference for monte carlo objectives. In *Int. Conf. Mach. and Learn.*, 2188–2196 (2016).
35. Van der Maaten, L. & Hinton, G. Visualizing data using t-sne. *J. Mach. Learn. Res.* **9** (2008).